Post-Print of: Environmental Pollution Volume 174, March 2013, Pages 134–141

Behaviour of Au-citrate nanoparticles in seawater and accumulation in bivalves at environmentally relevant concentrations

C.A. García-Negrete (a), J. Blasco (b), M. Volland (b), T.C. Rojas (a), M. Hampel (b), A. Lapresta-Fernández (a), M.C. Jiménez de Haro (a), M. Soto (c), A. Fernández (a)

a Instituto de Ciencia de Materiales de Sevilla (CSIC – Univ. Sevilla), Avda. Américo Vespucio nr. 49, CIC Cartuja, 41092 Sevilla, Spain

b Instituto de Ciencias Marinas de Andalucía (ICMAN-CSIC), Campus Universitario Río San Pedro, 11519 Puerto Real (Cádiz), Spain

c Zoology and Cell Biology Dept., Science and Technology Faculty, University of the Basque Country, Sarriena auzoa Z/G, 48940 Leioa-Bizkaia, Basque Country, Spain

Abstract

The degree of aggregation and/or coalescence of Au-citrate nanoparticles (AuNPs, mean size 21.5 ± 2.9 nm), after delivery in simulated seawater, are shown to be concentration-dependent. At low concentrations no coalescence and only limited aggregation of primary particles were found. Experiments were performed in which the marine bivalve (Ruditapes philippinarum) was exposed to AuNPs or dissolved Au and subsequently, bivalve tissues were studied by Scanning and Transmission Electron Microscopy and chemical analyses. We show that the bivalve accumulates gold in both cases within either the digestive gland or gill tissues, in different concentrations (including values of predicted environmental relevance). After 28 days of exposure, electron-dense deposits (corresponding to AuNPs, as proven by X-ray microanalysis) were observed in the heterolysosomes of the digestive gland cells. Although non-measurable solubility of AuNPs in seawater was found, evidence is presented of the toxicity produced by Au3+ dissolved species (chloroauric acid solutions) and its relevance is discussed.

Keywords

Gold nanoparticles; Chloroauric acid; Ecotoxicity; Sea water; Bivalve accumulation; Electron microscopy; Ruditapes philippinarum; Cellular location

1. Introduction

Gold nanoparticles (AuNPs) are already in use or being widely researched for numerous applications, ranging from biosensors to catalysts, in electronics, new paints and cosmetics and in cancer treatments, among others. Their unique properties, chemical stability, and their capacity to exhibit a multiplicity of shapes, particle sizes, and surface chemistry (Daniel and

Astruc, 2003; Cobley et al., 2011; Gonzalez et al., 2011; Henry et al., 2011) will ensure that they will be key nano-scale components in many twenty-first century technologies. Because of their prospective widespread use, AuNPs will almost certainly account for a considerable and persistent nanomaterial input to environmental systems (Lapresta-Fernández et al., 2012). Bivalve molluscs (Canesi et al., 2012) and other invertebrates (García-Alonso et al., 2011) are recognized biological monitors. In particular marine bivalves have the ability to concentrate a dissolved or suspended contaminant that may be present in low concentrations in the water media (Doherty, 1990) and there is increasing interest in obtaining new information about the potential toxic effects of NPs in bivalve species (Baun et al., 2008; Gomes et al., 2011; Canesi et al., 2012), and about the behaviour of NPs in aqueous media in environmental conditions (Nowack and Bucheli, 2007; Canesi et al., 2012; Lapresta-Fernández et al., 2012; Thio et al., 2012).

It has recently been demonstrated that 10 nm amine-functionalized AuNPs penetrate the gills and digestive epithelia of Corbicula fluminea, in experiments conducted in fresh water (FW) (Renault et al., 2008). Moreover, recent investigations have reported that biofilms and clams are the primary compartments in which surfactant-stabilized gold nanorods added to estuarine mesocosms accumulate (Ferry et al., 2009). In seawater (SW), the effects attributable to citrate- and didodecyl-dimethyl-ammonium bromide-stabilized gold NPs have been related to oxidative stress and general toxicity in the bivalve Mytilus edulis (Tedesco et al., 2010a and Tedesco et al., 2010b). In addition, a strong dependence on particle size was reported in these papers, with the smallest NPs being the most toxic (Tedesco et al., 2010b). Recently, Hull et al. (2011) have warned that nanoparticles resistant to salt-induced aggregation are anticipated to be persistent in aquatic ecosystems and these authors have shown, for serum-albumin functionalized AuNPs, that primary particle size can influence uptake and fate of nanoparticles in marine bivalves. Previous studies have revealed that citrate-capped AuNPs show a salt-induced aggregation behaviour that can also be reduced by functionalization of the NPs surface (Stakenborg et al., 2008). Based on data from the literature (Stakenborg et al., 2008; Su and Kanjanawarut, 2009; Zhang et al., 2012), citrate-capped AuNPs are likely to aggregate in the presence of electrolytes at concentrations much higher than environmentally relevant levels, but little is known about the salt-induced aggregation behaviour of these particles at lower concentrations.

In order to obtain useful information from trials in which marine bivalves are exposed to AuNPs, the behaviour of nanoparticles with respect to aggregation and/or coalescence, as well as solubility, in the media after delivery needs further clarification. More work is also required in conducting studies under environmentally-relevant conditions. Information available on the current levels of AuNPs in aquatic media is very limited, but recent predictions by Boxall et al. (2007) and Tiede et al. (2009) gave concentrations (referring to gold content) of 0.1 μg L−1 in water and 5.99 μg kg−1 in soil for engineered AuNPs originating from use in consumer products. Therefore, in the present paper, we first report a study of the physico-chemical evolution of citrate-stabilized AuNPs (in this paper referred as AuNPs) when delivered to artificial SW media, under both high and low relevant concentrations ranging from ppm to ppb levels. Surface Plasmon Resonance (SPR) and Scanning and Transmission Electron Microscopy (SEM and TEM) analyses are presented to draw conclusions regarding aggregation vs. coalescence of the particles. Secondly, we report the results related to the exposure of the

bivalve Ruditapes philippinarum not only to AuNPs but also to dissolved Au in SW, aiming to add a comparative dataset regarding possible toxicity mechanisms of AuNPs. New results are presented in this paper in relation to the location and distribution of Au in the clam tissues, using SEM, TEM and chemical analysis, together with findings on the damage induced in these tissues. In some of the bioaccumulation analyses it was even possible to get data from exposure experiments at 6 ppb levels, equal to the total predicted values in the Tiede et al. (2009) paper. Nevertheless for other experiments, higher concentrations were tested considering the detection limits of the available techniques.

2. Materials and methods

2.1. AuNP suspensions

2.1.1. Preparation

AuNPs suspensions with a concentration of 300 mg L−1 (as Au) were prepared following a procedure based on the synthesis method of Frens (Frens, 1972) although using higher concentrations. Specifically, 0.031 g of HAuCl4·3H2O (Aldrich, 99.9%) were dissolved in 50 mL of MilliQ® in a 100 mL round bottomed flask and heated to boiling under reflux conditions. Then 0.052 g of sodium citrate (Sigma–Aldrich, 99%), dissolved in 1 mL of MilliQ® water, were added and the solution was allowed to stand for 10 min for the reduction of the gold precursor; in the final suspension a wine-purple colour remains. From this starting solution, dilutions were made immediately after preparation, without allowing the colloid to age. With the objective of identifying possible macroscopic or microscopic effects, dilutions at both, medium (levels of mg L−1) and low concentrations (levels of μg L−1), were tested.

For the preparation of a medium-level concentration, the 300 mg L−1 citrate-stabilized AuNP suspension was diluted to a 30 mg L−1 concentration in standard SW, and in MilliQ® water, for comparison purposes. For the preparation of low-level concentrations, the 30 mg L−1 AuNP suspension was diluted in the range 6–600 μg L−1, again in both standard SW and MilliQ® water, according to the required concentration in each particular case throughout this study.

2.1.2. Characterization

AuNP suspensions were characterized by UV-VIS spectroscopy (Perkin Elmer Lambda 12) and transmission electron microscopy (TEM) or field emission gun scanning electron microscopy (FEG-SEM). Primary particle size and morphology were characterized using either a TEM microscope (Philips CM200) operating at 200 kV or a SEM-FEG microscope (Hitachi S-4800) operating at 30 kV. For sample preparation, 5–10 μL of a particular AuNP suspension was pipetted onto a carbon coated copper TEM grid and left to dry in air. The SEM-FEG instrument is also equipped with an adequate detector and a sample holder for copper grids so that SEM images were acquired in transmission mode.

2.2. Assays with R. philippinarum exposed to AuNP suspensions

Adult clams (Ruditapes philippinarum) of between 4.4 and 3.2 cm shell length (maximum axis) were supplied by a commercial clam aquaculture facility (Amalthea S. L., Chiclana, Spain). Acclimation took place in free-flow tanks for one week before starting the exposure. The

experiment was carried out in a semi-static water system at a ratio of one individual per litre of SW. For the course of the experiment, 25 individuals were placed in each of two series of tanks with 25 L of filtered SW (salinity 34, temperature 20 ± 0.7 °C, pH 8.13 ± 0.37), containing 6 and 30 μg L−1 of AuNPs respectively. For comparative purposes, clams were exposed to an ionic gold treatment in the form of Au3+ (chloroauric acid solution) at a concentration of 50 μg L−1 (as Au). Aliquots from a stock solution of Au (1000 mg L−1, certiPUR® standard, HAuCl4 in HCl 7% Merck) were added to the experimental tank directly. A control series without extra Au was run in parallel. Each experimental setting was conducted in duplicate. The exposure treatments were labelled as follows: Au3+ for dissolved gold and NP6 and NP30 respectively for 6 and 30 μg L−1 (as Au) of AuNPs. Aeration at the bottom of the tank was used to minimize agglomeration and subsequent sedimentation of the contaminants, and ∼100% of the media was changed every 48 h. For the duration of the experiment (28 days), clams were fed with 50 mL of algae solution (Isochrysis galbana, family: Rymnesiophyceae, 12 × 106 cell/ml) per tank, every 48 h, 2 h prior to the media change. Test animals were checked daily. Dead specimens were replaced in order to maintain a consistent organism: water volume ratio.

2.3. Analysis of gold in SW and tissue samples

Gold concentration in SW was assessed at 0 h (immediately after the first dose of contaminant) and 48 h (prior to feeding and the change of media) by Inductively-Coupled Plasma Mass Spectrometry (ICP-MS) (Thermo Serie X7) (Allabashi et al., 2009). Ten millilitre of SW media was collected for gold analysis, and 10 μL of HNO3 at 65% was added; and the sample was stored at −20 °C until analysis. Metal content in the digestive gland and gills tissue samples was also analysed using ICP-MS following procedures similar to well-established methods (Amiard et al., 1987; Renault et al., 2008; Allabashi et al., 2009). Clams were dissected over ice, recording the weight of the soft tissue (wet weight) for each specimen. Pooled (3 individuals) gill and digestive glands were frozen in liquid nitrogen and stored at −80 °C immediately after sampling. Frozen tissue samples were powdered in liquid nitrogen with the aid of a Cellcrusher (Stratech Scientific Ltd.). Aliquots of the frozen powder obtained were stored separately at −80 °C prior to homogenization and analysis. Tissue samples were homogenized by digestion with 2 mL 10.3 M HNO3 for 60 min at 95 °C, utilizing a digestion system (DigiPREP MS, SCP Science, France). Samples were topped up to final volume of 5 mL with MilliQ® water. All reagents were of supra pure quality. The results are expressed in μg g−1 wet weight. Comparative experiments were carried out on gill tissues using aqua regia in order to test the effectiveness of digestion/homogenization with HNO3 alone and similar results were obtained under the tested experimental conditions.

For statistical analysis accumulation data were transformed (log 1 + n) to homogenise the variance. Statistical differences for accumulation in the two tissues analyzed were tested by two-way ANOVAs (factors: time and exposure). The Scheffe test was used for post-hoc comparisons. A significance level of $p = 0.05$ was selected for all statistical tests.

2.4. Lipid peroxidation measurements

Lipid peroxidation was assessed by determining levels of malonaldehyde (MDA) following the methodology of Shaw et al. (2004), using 1-methyl-2-phenylindole and calculated against a MDA standard curve. Tissue MDA levels were derivatised in a 1 mL reaction mixture containing

a final concentration of 6.7 mM of 1-methyl-2-phenylindole (dissolved in acetonitrile), 2.3 mM of methanosulphonic acid, 100 µL of water and equal volume of sample diluted in homogenization buffer (1:4 v/v) or standard (10 mM 1,1,3,3-tetramethoxypropane, in 20 mM Tris–HCl, pH 7.4). The sample mixtures were vortexed and incubated at 45 °C for 40 min. The samples were cooled on ice and centrifuged at 15,000 g for 10 min at 4 °C. The supernatants were collected and read at 590 nm (Tecan F200). Results are expressed in MDA µmol min−1 mg−1 protein.

2.5. Subcellular localization of AuNPs taken up

The preparation of samples for the transmission electron microscopy (TEM) was performed following the methodology by Distel and Felbeck (1987) as modified by the "Centro de Investigación, Tecnología e Innovación" (CITIUS), University of Seville (Spain). At the end of the exposure period, clams were dissected over ice. Gills and digestive gland were cut into sections of ∼1 mm squares and fixed in cold 0.1 M sodium cacodylate trihydrate buffer solution (pH = 7.4) containing 2.5% of glutaraldehyde for 2.5 h at 4 °C. After that, samples were washed three times in a sodium trihydrate cacodylate buffer solution (pH = 7.4) for 5 min each and stored at 4 °C. Samples were post-fixed in 1% osmium tetroxide for 1 h at 4 °C, rinsed in buffer solution (3 times), containing 7.5% sucrose, for 20 min. Samples were then dehydrated at 4 °C in acetone (30, 0 and 70% acetone baths for 15 min each). Afterwards, samples were rinsed in 70% acetone bath containing 2% uranyl acetate for 4 h for pre-staining, and dehydrated once in 90% acetone (30 min), and twice in 100% acetone (15 min each). Embedding in Spurr's resin was performed at the same temperature (4 °C) with acetone/resin mixtures of 3:1 for 1 h, 1:1 for the second hour, and 1:3 for the third hour, followed by embedding in pure resin for 12 h. Samples were polymerized at 70 °C for a period of 7 h. Finally, semi and ultrathin sections (300 and 80 nm) were cut with an ultramicrotome (Leica EM UC7) using a diamond knife and placed on a carbon-coated copper TEM grid. Ultrathin sections were typically imaged with a Philips CM10 TEM microscope at an acceleration voltage of 80 kV. Detailed studies of Au location and distribution in the selected clam tissues were carried out in a Philips CM200 TEM microscope carefully aligned at an acceleration voltage of 80 kV and coupled to an EDS microprobe (EDAX DX-4). In addition to TEM analysis with ultrathin sections (80 nm thick), studies by SEM-FEG were performed in a Hitachi S4800 microscope also coupled to an EDS probe (Bruker, XFlash 4100) and equipped with a transmission mode detector that allowed working with semi-thin samples (300 nm slices) at 20 kV.

3. Results and discussion

3.1. Physico-chemical evolution of citrate-stabilized AuNPs in SW media

In order to assess the behaviour of the AuNPs after release into a seawater environment, a thorough characterization of nanoparticle suspensions after diluting to a mass-normalized concentration of 30 mg L−1 (as Au) is needed, even though this concentration is higher than environmentally-relevant concentrations (Tiede et al., 2009; Lapresta-Fernández et al., 2012). Different macroscopic aspects were observed depending on the chemical nature of the final water reservoir. Thus, at a concentration of 300 mg L−1 the suspension showed a dark purple colour (Fig. 1a) whereas after diluting up to 30 mg L−1, it exhibited either the typical red colour in MilliQ® water (Fig. 1b), due to the localized surface plasmon resonance (SPR) as presented in

Fig. 1c (UV-Vis absorption spectra in b. plot), or a weak violet colour in artificial SW (Fig. 1d) associated with higher inter-particle interactions, as reflected in both the intensity loss and the red-shift of the SPR signal (Fig. 1c, UV-Vis absorption spectra in d. plot). It should be noted that the 30 mg L−1 AuNPs suspension in artificial SW evolves leading to a macroscopic precipitation and a colourless supernatant within the following 4 h (Fig. 1e); this outcome indicates the formation of aggregates and complete disappearance of the SPR phenomena, whereas the 30 mg L−1 AuNP colloidal suspension in MilliQ® water is highly stable, showing nearly spherical particles (average diameter, d = 23.5 ± 2.8 nm following a Lognormal fitting of the size distribution histogram) as presented in Fig. 1f–g. The reproducibility on particle size for the 30 mg L−1 AuNP colloidal suspension in MilliQ® water was tested by light scattering and TEM for each batch.

In the case of AuNP suspensions of 60 μg L−1, which is a concentration only one order of magnitude above predicted environmentally relevant values (Boxall et al., 2007; Tiede et al., 2009), a contradictory behaviour to that observed at high concentration was found. No precipitation occurs in suspensions at this concentration either in MilliQ® water or in artificial SW. On the other hand representative TEM shows that small agglomerates can be formed. In comparison with agglomerates found in MilliQ® water (Fig. 2a), those corresponding to artificial SW are clearly bigger in size (Fig. 2b), however no important differences in morphology and size were found for primary particles from any of the different aqueous media (Fig. 2a–b). Most importantly, no coalescence of particles seems to occur in the case of artificial SW agglomerates, as might be expected. The above discussion suggests that depending on the final concentration in the SW media, citrate-stabilized AuNPs can be considered as “nanoparticles resistant to salt-induced aggregation” and can be proposed indeed as a model contaminant for ecotoxicology studies at concentrations more similar to those relevant in the natural environment. At this level of dilution the extinction coefficient of the SPR absorption is not sufficient to obtain any information. Neither are other techniques like DLS (dynamic light scattering) feasible at these concentrations. The TEM images presented here are representative of many analyses carried out on the samples, and have proved to be very useful for studying the evolution of the AuNPs in the SW media, at concentrations of interest. The key point for the interpretation of the data is the fact that both samples (Fig. 2a–b), those prepared in MilliQ® and in SW, are of the same concentration and were processed in the same way for comparison purposes. Further attempts to reduce the concentration of AuNPs more closely to the estimated environmental concentration (Boxall et al., 2007; Tiede et al., 2009) would be out of the range for a feasible TEM analysis, and very probably would not change the conclusions regarding the absence of coalescence.

In the case of citrate-stabilized AuNPs dispersed at the 600 μg L−1 concentration in artificial SW, fine sediment is found after two days; however, the sediment re-disperses well through manual agitation. This behaviour could be understood in terms of the microstructure of the agglomerates formed. As Fig. 2c shows, the 600 μg L−1 AuNP suspension in artificial SW is made up of large agglomerates due to the appreciable ionic strength; however, limited coalescence between primary particles makes it possible to dissociate assemblies through agitation. The panel (d) in Fig. 2 shows the particle size distribution histogram obtained from the TEM analysis of the sample dispersed at the 600 μg L−1 concentration. An average particle size of 21.5 ± 2.9 nm was obtained, in agreement with that reported in Fig. 1f–g. It should be

noted that different AuNP concentrations in artificial SW lead to different macroscopic behaviour as a result of the different balance between aqueous media ionic charges and the surface potential of citrate-stabilized gold particles.

As we will demonstrate in following paragraphs, dissolved ionic gold in the form of Au3+ (chloroauric acid solution) appears to be strongly toxic for the bivalves under study. In this context we also investigated the solubility of AuNPs in the artificial SW. To determine the concentration of dissolved ionic Au species in suspensions of AuNPs, ultra-filtration was undertaken using Vivaspin 20 filters (3000 MWCO). The filtered solution of the 60 ppm AuNPs suspension in MilliQ® water, prepared as described, gives a dissolved Au concentration of 60 ppb by ICP-MS analysis, indicating that ca. 0.1% by wt of precursor gold salt could remain un-reduced after synthesis. Ultra-filtration was also carried out after dilution of the original 60 ppm Au NP suspension with artificial SW to a 30 ppb suspension from time 0 up to 48 h after dilution. In all cases the filtered solutions lead to an undetectable Au signal by ICP-MS, indicating that the gold concentration is below the actual detection limit of 0.05 ppb; this also demonstrates that solubility of the AuNPs is unlikely under the reported experimental conditions. Therefore the results reported below constitute a set of comparative data where independent effects for ionic gold and AuNPs are reported.

3.2. Gold bioaccumulation in bivalves

Assays of bivalve exposures to AuNPs (6 and 30 μg L−1 of gold) and ionic Au3+ (50 μg L−1 of gold) were carried out, together with control experiments. The concentration chosen of 50 μg L−1 for Au3+ corresponds to a value below the previously reported minimum values showing toxicological effects in algae (Robinson et al., 1997); while the minimum gold concentration (6 μg L−1) for AuNPs is just below the predicted value (6.13 μg L−1 including water and soil) in the environment (Boxall et al., 2007; Tiede et al., 2009). Analyses of clam tissue samples by ICP-MS are summarized in Fig. 3a–b; ANOVA multifactorial analysis provided evidence in both target tissues that exposure and time factors had a significant effect on accumulation. Trace amounts of gold for the control experiments are within the experimental errors and are considered as zero values. Gold was significantly accumulated in both the digestive gland and gills already after 3 h of exposure (Fig. 3a–b). However, AuNPs accumulated more in the digestive gland, while Au3+ accumulated more in gills (Fig. 3a–b). The preferential accumulation of AuNPs is likely via capture and ingestion. NPs are directed into tubules of the digestive glands and potentially taken up by endocytosis. Other routes as gills, mantle and labial pals are considered less important for NPs accumulation (Canesi et al., 2012). In Corbicula fluminea, bovine serum albumin gold nanoparticles were also confined to digestive gland and digestive tract regions, with little migration to other systems (Hull et al., 2011). Even so, increased accumulation was reported in the digestive glands of M. edulis exposed to gold-citrate NPs (Tedesco et al., 2010a). Others authors (Gomes et al., 2011) found also that copper concentration was higher in gills for dissolved species, in comparison with CuO nanoparticles, in mussels exposed to both treatments.

Despite the considerable variability observed within groups, certain general trends can be seen in Fig. 3a from analysis of the digestive gland sample, depending on the exposure time. The Scheffe post-hoc test (at $p < 0.05$) showed significant differences between the accumulation

for the initial six hours exposure, and samples collected after seven days. For the NP30 treatment, an initial response was found whereby Au concentration increases in this organ during the first 24 h. Afterwards, Au concentration was nearly stationary up to the assay limit of 28 days of exposure (Fig. 3a). Gold concentration found in the digestive gland after exposure to NP6 was much less than after exposure to NP30 as expected for the higher concentration in this experiment. In the case of NP6, concentrations increased to reach a maximum after 12 h, with similar levels being maintained between 12 h and 28 days of exposure (Fig. 3a).

Another approach to studying accumulation behaviour is to analyze gold removal in the water column. Using this methodology other researchers (Hull et al., 2011) have suggested three consecutive phases to describe filtering and removing of gold NP contaminants by an Asian clam (C. fluminea) as follows: first, the initial logarithmic phase that is attributable to the acclimation period required for the clams to begin filtering following transfer to the assay chamber; second, a linear clearance phase that is representative of a period during which the clams have acclimated to the assay environment and begun actively filtering; and third, a levelling-off phase that may be the result of a combination of factors, including decreasing particle concentration, compaction of the digestive tract or physiological adjustment of the filtering and ingestion rate. In addition we cannot presently exclude the possibility that accumulation in R. philippinarum can be affected by gold sorption over the surfaces of the treatment tank, or gold sorbed to algal cells during feeding, but these possibilities were outside the scope of the present investigation. In the case of the digestive gland, the physiological adjustment of filtering and ingestion/release rates could be the reason for the dose-dependent accumulation levels observed here, and in particular for the nearly stationary last phase in the NPs treatments. In any case, for NP30, accumulation occurring in all phases is between 2 and- 3 times higher than the accumulation values for NP6. On the other hand, the highest Au concentration level for the whole exposure period and all treatments is recorded for the NP30 treatment after 24 h of exposure (Fig. 3a).

Gold accumulation within the digestive gland produced by the Au3+ treatment was lower than the values produced by both NP concentrations tested (Fig. 3a). Moreover, accumulation of Au after exposure to Au3+ was delayed in comparison with that for the NPs, and after a slow initial accumulation, increased with exposure time up to the end of the exposure period (Fig. 3a). It seems that the chemical nature of the contaminant has an effect on the duration and complexity of the initial phase: in digestive gland Au accumulation with NPs takes place more rapidly and reaches higher values, compared with that in the Au3+ treatment. For this treatment Au accumulation behaviour shows a nearly stationary second phase between 24 h and 7 days, and an increase after 7 days that differs markedly from that observed in the nanoparticle treatments, where the last phase followed a nearly stationary trend. Of particular interest, as shown below for the Au3+ treatment, is the fact that this contaminant showed a strongly toxic nature, being capable of directly affecting the adjustment of the organism's filtering and ingestion rate. Thus, the accumulation behaviour observed for Au3+ may be conditioned, in part, by this toxic nature of the contaminant. Different behaviours for gold accumulation, as a function of the contaminant, can also be inferred from variations in gold concentration in the water column for the different treatments (Supplementary file Fig. S1). Fig. 3b also shows a strong accumulation of gold in gill tissue samples after exposure to Au3+.

3.3. Responses in bivalves to AuNPs and their commonly-used precursors

The exposure to Au in the different forms tested produced dissimilar responses regarding mortality endpoints. NP6 and NP30 treatments did not produce any significant effect in mortality, compared with control treatments. However, a severe mortality rate was recorded after the Au3+ treatment (Table 1). This effect is of special concern with respect to the disposal of specific nanoparticle precursors in the manufacturing of engineered nanoparticles. Chloride can be ruled out as toxicity source because the experiments have been carried out in seawater with a salinity of 34 which represents ca. 20 g Cl^- per kg of SW media.

TEM micrographs of control samples do not reveal any ultrastructural disturbance in cells of the digestive gland (Fig. 4a) suggesting a good health status. In the case of the Au3+ treatment the ultrastructural analysis revealed histopathological effects in all the samples tested. Fig. 4b shows large areas which were completely disrupted with clear signs of cell damage (i.e. altered nuclear membranes). Additionally, some mitochondria lost their typical morphology exhibiting a swollen profile and alteration in the inner membrane with absence of cristae (Fig. 4b). Furthermore the NP30 treatment was also able to produce areas with morphological alterations (see disrupted membrane in the bottom-right area of Fig. 4c). We cannot however exclude the possibility that the observed alteration could have been produced during sample preparation as additional TEM and FEG-SEM micrographs show good health status of the tissues after the AuNP treatments (see Supplementary file Fig. S2a–b).

Additional information about possible toxic effects of either or both AuNPs and Au3+ on the marine bivalves can be inferred from early oxidative stress effects as expressed by lipid peroxidation (see Supplementary file Fig. S3). Results from the experiments performed only showed a significant increase in the oxidative stress indicator for the Au3+ exposure assays, as compared to controls, during the first 3 h, and a modest remaining increase at other sampling points up to 24 h. In the case of AuNPs, all tested treatments only caused modest oxidative stress, as compared to controls, at sampling points up to 12 h, any further oxidative stress being unlikely during the next 12 h. In a previous study, exposure of the mollusk Mytilus edilus to ~5 nm AuNPs over 24 h showed significant increase in oxidative damage, as expressed by lipid peroxidation at concentrations of 750 μg L^{-1} (Tedesco et al., 2010b), whereas AuNPs of ~15 nm, at identical concentration, only caused modest oxidative stress (Tedesco et al., 2010a). As an interpretation of the different responses, the toxic effect has been attributed principally to the size-related oxidative properties of AuNPs (Tedesco et al., 2010b). In the current study the clear increase in the oxidative stress indicator, as measured for the assays of exposure to Au3+, corroborates again the toxic effects of this contaminant in the bivalves. On the other hand, the lipid peroxidation results for treatments with AuNPs do not seems to reveal a behaviour different from that previously obtained in other bivalve exposure experiments (Tedesco et al., 2010a). The current study also corroborates the view that the specific chemical stability of the metal (dissolved or nanoparticulate) is a main parameter affecting cellular toxicity, as previously suggested (Auffan et al., 2009). Studies with gold NPs of smaller sizes or the effect of gold reduction by co-dissolved organic matter may be relevant in future investigations.

3.4. Cellular localization of AuNPs taken up by organisms

Recently Hull et al. (2011) tried to verify that gold is internalized by bivalves (C. fluminea) using a synchrotron-based XRF microscope. The high spatial resolution of the technique (beam size of 3 μm × 3 μm) allowed the localization of diffusely distributed gold spots at the digestive gland and regions of the digestive tract. However, this work provided limited information about the form that AuNPs take during digestion since if gold NPs are digested then changes in particle size, shape, or aggregation state should be expected. Thus, the localization of internalized AuNPs is a difficult question to resolve, even in the case of engulfment in organelles responsible for intracellular digestion, i.e. in digestive cell lysosomes.

Present observations of digestive gland tissue for the NP30 treatment using TEM reveal that NPs were directed to digestive cell lysosomes, and more precisely to lysosomes and residual bodies inside them (Fig. 4c). In the high magnification TEM micrograph illustrated in Fig. 4d, a residual body released into the lumen of the digestive tubule can be observed bearing electron-dense granules (inside the marked areas). The residual body, or heterolysosome, exhibited a semi-digested material that, according to EDS analysis (Fig. 4e) corresponded to elemental gold (Os and U were added during sample preparation, and Cu belongs to the TEM grid). It is likely that, AuNPs present in green algae, as a vector to the clam C. fluminea, produced electron-dense granules located in a vacuole (lysosomal nature) that was later incorporated in the gills and the digestive epithelia (Renault et al., 2008). However, those authors did not prove the elemental composition of these granules, as has been proved in the present work. It should be noted that this is the first confirmation of the location of AuNPs associated with digestive cell lysosomes in R. philippinarum after exposure to NPs in seawater. It is also interesting to note that AuNPs associated with the heterolysosome exhibited a marked coalescence (Fig. 4d) that leads clearly to aggregates/particles larger than those in the working solutions (Fig. 2b). Additional confirmation of accumulation of AuNPs in the digestive gland tissue can be found in Fig. 5(a and b) as measured by FEG-SEM in transmission mode. Although it was not the aim in this paper to study particle size effects, the results in Fig. 4d may indicate a certain preferential accumulation for the larger particles/aggregates, as proposed by Hull et al. (2011). The effect here however is more likely to be due to cellular digestion.

In a similar way, gold accumulation was also demonstrated in gills by ICP-MS analysis (Fig. 3b). In addition, the combination of both FEG-SEM and TEM analysis allowed the ultrastructural location and identification of electron-dense granules in gill cells after the NP30 treatment (Fig. 5c). These electron-dense granules exhibited a shape and size similar to that of the AuNPs dosed as contaminant, but EDX did not confirm the gold nature of their composition (Fig. 5d). TEM analysis showed that electron-dense granules not containing gold were typically found associated with the extracellular matrix of gills tissues (Supplementary file Fig. S4a–b). EDX measurements are therefore strongly recommended to confirm the chemical nature of electron-dense granules.

4. Conclusions

Firstly, the results in this paper show that, at low measurable concentrations, AuNPs can be available in the seawater column due to their limited aggregation. Analysis of clam tissue samples by ICP-MS showed that gold accumulated significantly in both the digestive gland and

gills already after only 3 h of exposure to both AuNPs treatments and to Au3+ dissolved species (chloroauric acid solutions). AuNPs accumulated more in the digestive gland, whereas Au3+ accumulated more in gills.

Mortality studies have shown the high toxicity of soluble Au3+ precursor species. This effect is of special concern with respect to the disposal of specific nanoparticle precursors in the manufacturing of engineered nanoparticles. In our experiments gold solubility was not detectable under the reported experimental conditions, after 48 h of presence of AuNPs in the seawater media.

The combined TEM/EDX analysis allowed the accumulation of AuNPs to be localized unequivocally in the digestive gland cells, and more precisely in their lysosomal system. The location of AuNPs in heterolysosomes of digestive gland cells of Ruditapes philippinarum has been presented here for the first time. EDX measurements are therefore strongly recommended to confirm the chemical nature of electron-dense granules for future studies of the uptake of nanomaterials.

Acknowledgements

The authors gratefully acknowledge financial support from the Junta de Andalucía (FEDER PE2009-FQM-4554, TEP-217) and EU FP7 AL-NANOFUNC project (CT-REGPOT2011-1-285895). We would like to thank A. Fernández-Estefane of CITIUS for the preparation of TEM samples. We also thank ICMS and CITIUS for Electron Microscopy facilities.

References

Allabashi et al., 2009 R. Allabashi, W. Stach, A. de la Escosura-Muñiz, L. Liste-Calleja, A. Merkoçi

ICP-MS: a powerful technique for quantitative determination of gold nanoparticles without previous dissolving

Journal of Nanoparticle Research, 11 (2009), pp. 2003–2011

Amiard et al., 1987 J.C. Amiard, A. Pineau, H.L. Boiteau, C. Metayer, C. Amiard-Triquet

Application de la spectrometrie d'absorption atomique zeeman aux dosages de huit elements traces (Ag, Cd, Cr, Cu, Mn, Ni, Pb et Se) dans des matrices biologiques solides

Water Research, 21 (1987), pp. 693–697

Auffan et al., 2009 M. Auffan, J. Rose, M. Wiesner, J.-Y. Bottero

Chemical stability of metallic nanoparticles: a parameter controlling their potential cellular toxicity in vitro

Environmental Pollution, 157 (2009), pp. 1127–1133

Baun et al., 2008 A. Baun, N. Hartmann, K. Grieger, K. Kusk

Ecotoxicity of engineered nanoparticles to aquatic invertebrates: a brief review and recommendations for future toxicity testing

Ecotoxicology, 17 (2008), pp. 387–395

Boxall et al., 2007 Boxall, A., Chaudhry, Q., Sinclair, C., Jones, A., Aitken, R., Jefferson, B., Watts, C., 2007. Current and Future Predicted Environmental Exposure to Engineered Nanoparticles. Report to Department of Environment Food and Rural Affairs (Defra), Central Science Laboratory, York, 55 pp.

Canesi et al., 2012 L. Canesi, C. Ciacci, R. Fabbri, A. Marcomini, G. Pojana, G. Gallo

Bivalve molluscs as an unique target group for nanoparticle toxicity

Marine Environmental Research, 76 (2012), pp. 16–21

Cobley et al., 2011 C.M. Cobley, J. Chen, E.C. Cho, L.V. Wang, Y. Xia

Gold nanostructures: a class of multifunctional materials for biomedical applications

Chemical Society Reviews, 40 (2011)

Daniel and Astruc, 2003 M.-C. Daniel, D. Astruc

Gold nanoparticles: assembly, supramolecular chemistry, quantum-size-related properties, and applications toward biology, catalysis, and nanotechnology

Chemical Reviews, 104 (2003), pp. 293–346

Distel and Felbeck, 1987 D.L. Distel, H. Felbeck

Endosymbiosis in the lucinid clams Lucinoma aequizonata, Lucinoma annulata and Lucina floridana: a reexamination of the functional morphology of the gills as bacteria-bearing organs

Marine Biology, 96 (1987), pp. 79–86

Doherty, 1990 F.G. Doherty

The Asiatic clam, Corbicula spp., as a biological monitor in freshwater environments

Environmental Monitoring and Assessment, 15 (1990), pp. 143–181

Ferry et al., 2009 J.L. Ferry, P. Craig, C. Hexel, P. Sisco, R. Frey, P.L. Pennington, M.H. Fulton, I.G. Scott, A.W. Decho, S. Kashiwada, C.J. Murphy, T.J. Shaw

Transfer of gold nanoparticles from the water column to the estuarine food web

Nature Nanotechnology, 4 (2009), pp. 441–444

Frens, 1972 G. Frens

Controlled nucleation for the regulation of the particle size in monodisperse gold suspensions

Nature Physical Science, 241 (1972), pp. 20–22

García-Alonso et al., 2011 J. García-Alonso, F.R. Khan, S.K. Misra, M. Turmaine, B.D. Smith, P.S. Rainbow, S.N. Luoma, E. Valsami-Jones

Cellular internalization of silver nanoparticles in gut epithelia of the estuarine polychaete Nereis diversicolor

Environmental Science & Technology, 45 (2011), pp. 4630–4636

Gomes et al., 2011 T.N. Gomes, J.P. Pinheiro, I. Cancio, C.G. Pereira, C. Cardoso, M.J.O. Bebianno

Effects of copper nanoparticles exposure in the mussel Mytilus galloprovincialis

Environmental Science & Technology, 45 (2011), pp. 9356–9362

Gonzalez et al., 2011 E. Gonzalez, J. Arbiol, V.F. Puntes

Carving at the nanoscale: sequential galvanic exchange and kirkendall growth at room temperature

Science, 334 (2011), pp. 1377–1380

Henry et al., 2011 A.-I. Henry, J.M. Bingham, E. Ringe, L.D. Marks, G.C. Schatz, R.P. Van Duyne

Correlated structure and optical property studies of plasmonic nanoparticles

Journal of Physical Chemistry C, 115 (2011), pp. 9291–9305

Hull et al., 2011 M.S. Hull, P. Chaurand, J. Rose, M. Auffan, J.-Y. Bottero, J.C. Jones, I.R. Schultz, P.J. Vikesand

Filter-feeding bivalves store and biodeposit colloidally stable gold nanoparticles

Environmental Science & Technology, 45 (2011), pp. 6592–6599

Lapresta-Fernández et al., 2012 A. Lapresta-Fernández, A. Fernández, J. Blasco

Nanoecotoxicity effects of engineered silver and gold nanoparticles in aquatic organisms

TrAC Trends in Analytical Chemistry, 32 (2012), pp. 40–59

Nowack and Bucheli, 2007 B. Nowack, T.D. Bucheli

Occurrence, behavior and effects of nanoparticles in the environment

Environmental Pollution, 150 (2007), pp. 5–22

Renault et al., 2008 S. Renault, M. Baudrimont, N. Mesmer-Dudons, P. Gonzalez, S. Mornet, A. Brisson

Impacts of gold nanoparticle exposure on two freshwater species: a phytoplanktonic alga (Scenedesmus subspicatus) and a benthic bivalve (Corbicula fluminea)

Gold Bulletin, 41 (2008), pp. 116–126

Robinson et al., 1997 M.G. Robinson, L.N. Brown, B.D. Hall

Effect of gold(III) on the fouling diatom Amphora coffeaeformis: uptake, toxicity and interactions with copper

Biofouling, 11 (1997), pp. 59–79

Shaw et al., 2004 J.P. Shaw, A.T. Large, P. Donkin, S.V. Evans, F.J. Staff, D.R. Livingstone, J.K. Chipman, L.D. Peters

Seasonal variation in cytochrome P450 immunopositive protein levels, lipid peroxidation and genetic toxicity in digestive gland of the mussel Mytilus edulis

Aquatic Toxicology, 67 (2004), pp. 325–336

Stakenborg et al., 2008 T. Stakenborg, S. Peeters, G. Reekmans, W. Laureyn, H. Jans, G. Borghs, H. Imberechts

Increasing the stability of DNA-functionalized gold nanoparticles using mercaptoalkanes

Journal of Nanoparticle Research, 10 (2008), pp. 143–152

Su and Kanjanawarut, 2009 X. Su, R. Kanjanawarut

Control of metal nanoparticles aggregation and dispersion by PNA and PNA–DNA complexes, and its application for colorimetric DNA detection

ACS Nano, 3 (2009), pp. 2751–2759

Tedesco et al., 2010a S. Tedesco, H. Doyle, J. Blasco, G. Redmond, D. Sheehan

Exposure of the blue mussel, Mytilus edulis, to gold nanoparticles and the pro-oxidant menadione

Comparative Biochemistry and Physiology C – Toxicology & Pharmacology, 151 (2010), pp. 167–174

Tedesco et al., 2010b S. Tedesco, H. Doyle, J. Blasco, G. Redmond, D. Sheehan

Oxidative stress and toxicity of gold nanoparticles in Mytilus edulis

Aquatic Toxicology, 100 (2010), pp. 178–186

Thio et al., 2012 B.J.R. Thio, M.O. Montes, M.A. Mahmoud, D.-W. Lee, D. Zhou, A.A. Keller

Mobility of capped silver nanoparticles under environmentally relevant conditions

Environmental Science & Technology, 46 (2012), pp. 6985–6991

Tiede et al., 2009 K. Tiede, M. Hassellov, E. Breitbarth, Q. Chaudhry, A.B.A. Boxall

Considerations for environmental fate and ecotoxicity testing to support environmental risk assessments for engineered nanoparticles

Journal of Chromatography A, 1216 (2009), pp. 503–509

Zhang et al., 2012 X. Zhang, M.R. Servos, J. Liu

Surface science of DNA adsorption onto citrate-capped gold nanoparticles

Langmuir, 28 (2012), pp. 3896–3902

Figure captions

Figure 1. Macroscopic appearance of both (a) 300 mg L−1 AuNPs suspension and (b) the same suspension after dilution to 30 mg L−1 in MilliQ® water. (c) Extinction spectra of suspensions of 30 mg L−1 AuNPs corresponding to samples showed in panels (b) and (d). Macroscopic appearance of both: (d) freshly diluted suspension of AuNPs to 30 mg L−1 in artificial SW, and (e) its evolution after 4 more hours. (f) SEM-FEG image of sample designated in this figure as (b); particle sizes in the image were measured using the Digital Micrograph Gatan program, and the results are shown as a size distribution histogram of primary particles (panel g).

Figure 2. Representative TEM images showing microstructures of suspensions of AuNPs after dilution in different water media and concentrations: 60 µg L−1 in both (a) MilliQ® water and (b) artificial SW; 600 µg L−1 in (c) artificial SW. (d) Size distribution histogram for primary particles of a suspension of 600 µg L−1 AuNPs in artificial SW.

Figure 3. Au concentrations (µg g−1 wet weight) within (a) digestive gland tissue and (b) gill tissue, at different sampling points for the exposure treatments (HAuCl4 50 µg L−1(Au3+)) and AuNPs suspensions (6 µg L−1(NP6) and 30 µg L−1(NP30)). Data given as mean ± standard deviation for n = 2 replicates.

Figure 4. TEM images showing digestive gland tissue following 25 days of exposure with: (a) control; (b) HAuCl4 50 µg L−1 (Au3+) and (c) suspension of 30 µg L−1 of AuNPs (NP30). (d) High magnification TEM image showing the ultra-structure of the chosen region (marked area in panel c); (e) the corresponding EDX spectra of the electron-dense contrasts region (marked area in panel d).

Figure 5. FEG-SEM images: (a) digestive gland tissue and (c) gills tissue with attached EDX spectra in (b) and (d) for the marked electron-dense contrasts area in each image.

Table 1

Table 1. Mean clam mortality after 7, 14 and 28 days of exposure to the respective treatments ($HAuCl_4$ 50 µg L^{-1}(Au^{3+}) and gold NP suspensions (6 µg L^{-1}(NP6) and 30 µg L^{-1}(NP30)), plus control). Data given as mean ± standard deviation for $n = 2$ replicates. Initial individuals: 25 per separated experiment. Asterisk: the same value as obtained at day 7. For the days 14 and 28, mortality values for the Au^{3+} treatment were significantly different ($p < 0.05$).

Treatment	**Mortality (Individuals) as a function of the exposure time**		
	Day 7	**Day 14**	**Day 28**
Control	0.5 ± 0.7	*	*
Au^{3+}	3 ± 2.1	7.5 ± 0.7	8.0 ± 1.4
NP6	0.5 ± 0.7	*	*
NP30	0.5 ± 0.7	*	*

Figure 1

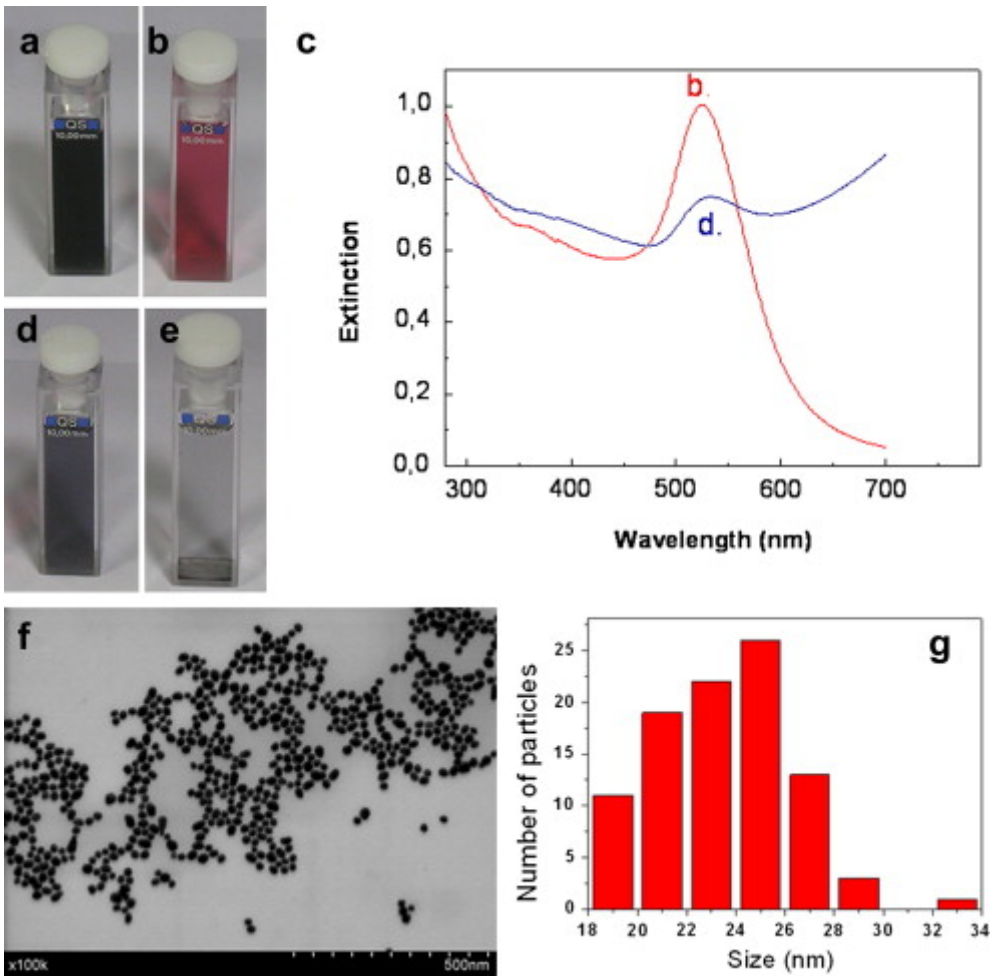
a
b
c
d
e
f
g
b.
d.
Extinction
Wavelength (nm)
Number of particles
Size (nm)
x100k
500nm

Figure 2

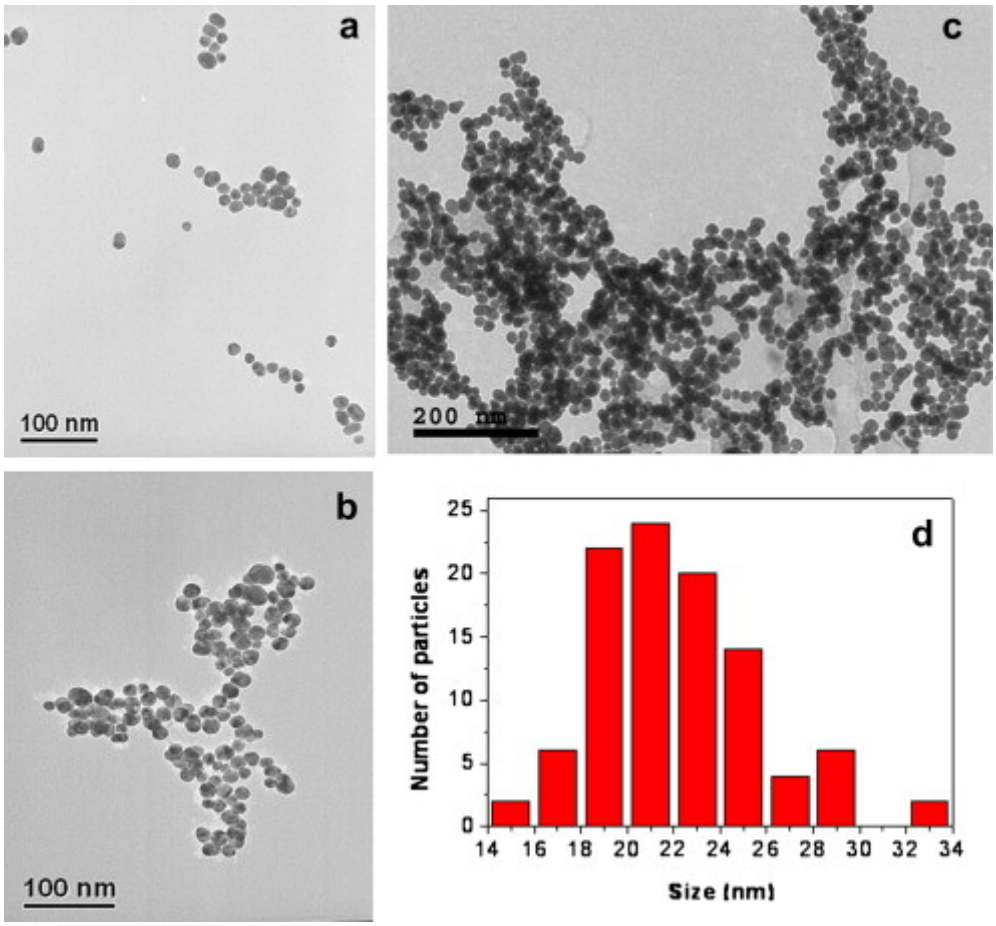
a
100 nm
c
200 nm
b
100 nm
d
Number of particles
Size (nm)
0
5
10
15
20
25
14
16
18
20
22
24
26
28
30
32
34

Figure 3

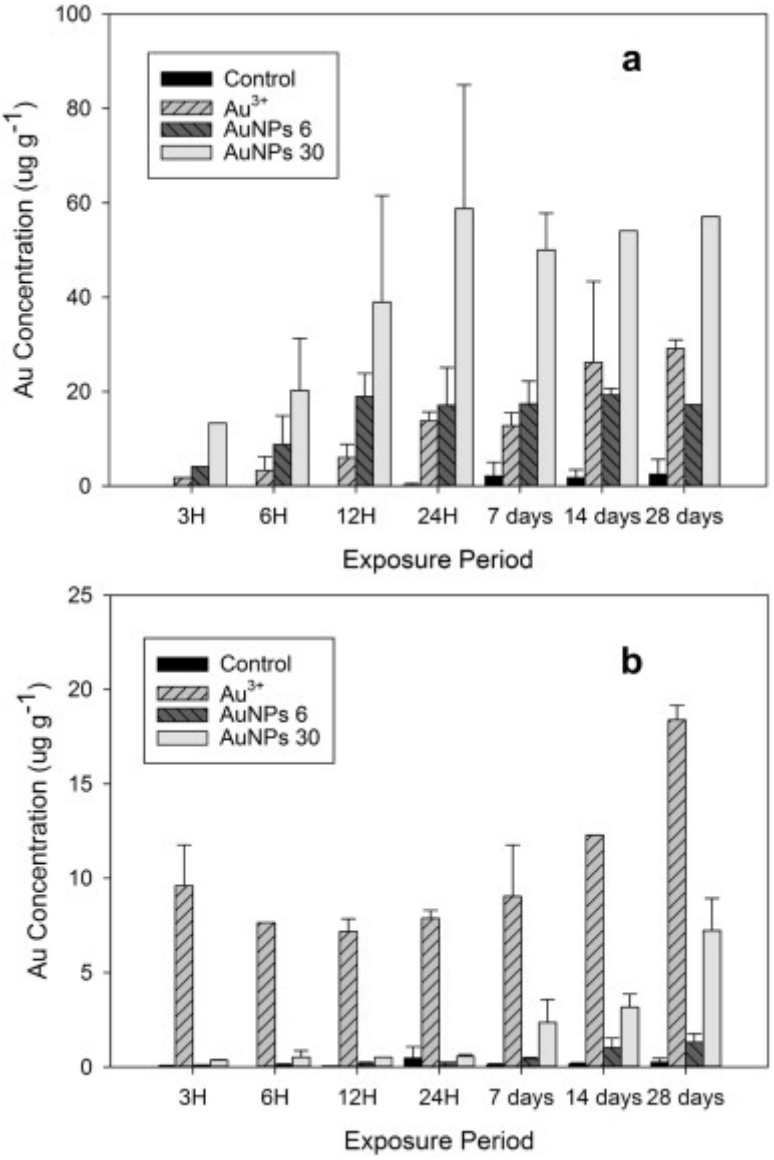
a
Control
Au3+
AuNPs 6
AuNPs 30
Au Concentration (ug g-1)
100
80
60
40
20
0
3H
6H
12H
24H
7 days
14 days
28 days
Exposure Period
b
Control
Au3+
AuNPs 6
AuNPs 30
Au Concentration (ug g-1)
25
20
15
10
5
0
3H
6H
12H
24H
7 days
14 days
28 days
Exposure Period

Figure 4

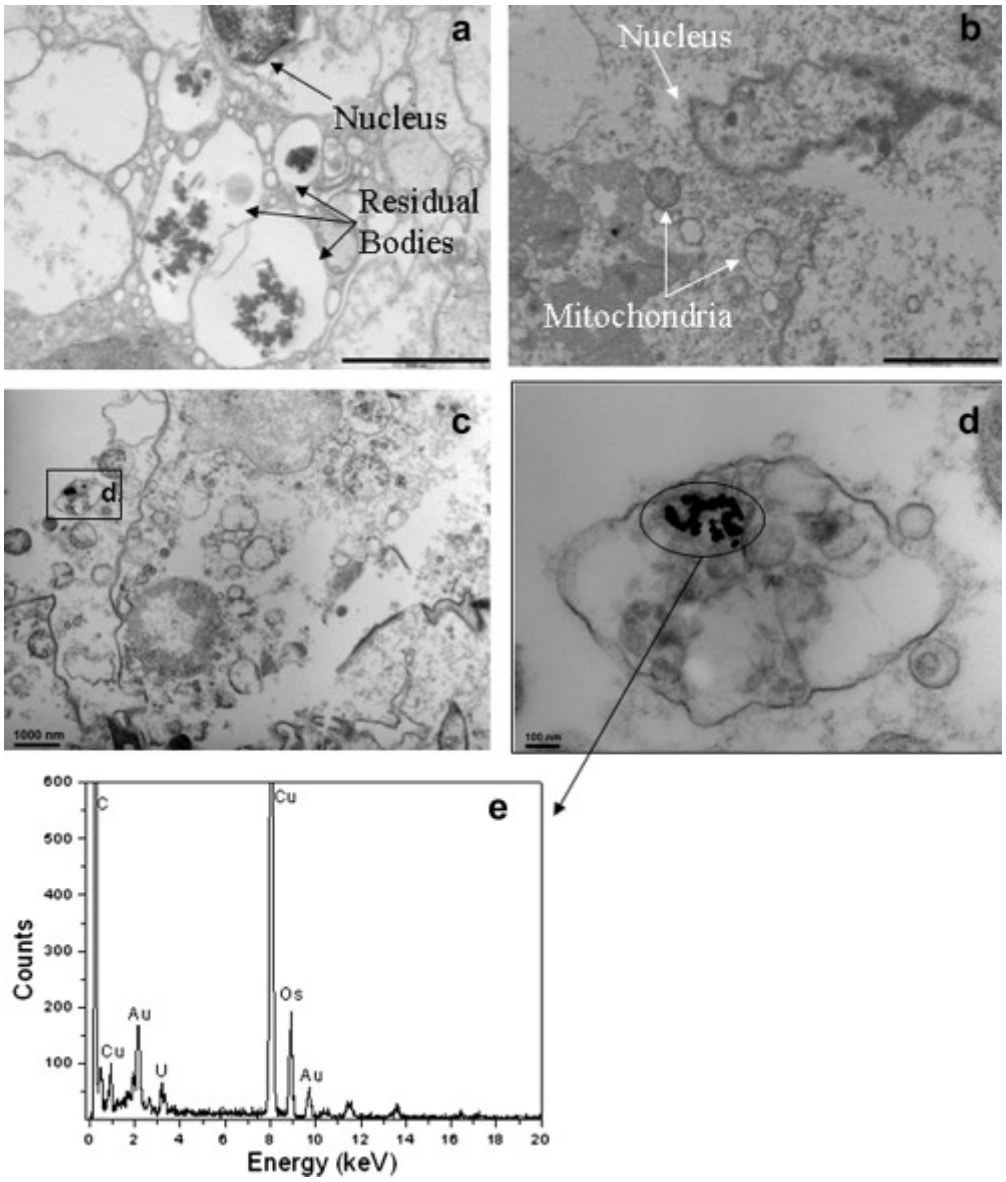
a
Nucleus
Residual
Bodies
b
Nucleus
Mitochondria
c
d
1000 nm
d
100 nm
e
Counts
Energy (keV)
C
Cu
Au
U
Cu
Os
Au

Figure 5

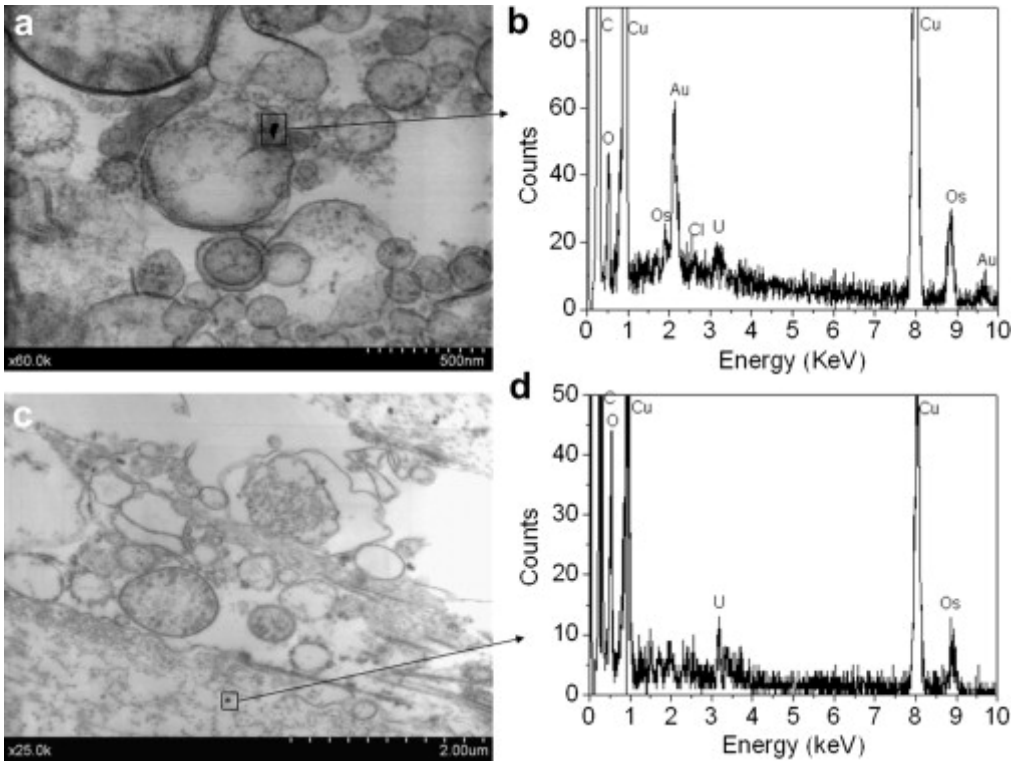
a
x60.0k
500nm
b
C
Cu
Au
O
Os
Cl
U
Cu
Os
Au
Counts
Energy (KeV)
c
x25.0k
2.00um
d
C
O
Cu
U
Cu
Os
Counts
Energy (keV)